SAR : multi-temporal pile (2)

M. Gostiaux Gabriel
M. Gabriel Gostiaux, Master of Science student, Institute of Optics, Palaiseau, 91 120, France
gabriel.gostiaux@institutoptique.fr

https:reacton-brew.com

Abstract: Synthetic Aperture Radar images can be acquired in a long time frame, allowing to compute interferences if the acquisition trajectories of the aircraft or satellite are identical between each acquisition. Those interferences helps in understanding changes in environments : biomass evolution along seasons, greenhouse emissions in urban zones, buildings and structure demolition or construction and even vehicule position. Another important aspect of SAR imaging concerns the polarimetry of the acquired images, which can be then used to classify lands according to their nature.

Keywords: SAR, multi-temporal pile, Polarimetry.
OCIS codes: (000.0000) General.

References and links

1. "Introduction à l'imagerie SAR", N. Trouvé, IOGS **SAR** (2024).

---

1. Introduction

The goal here is to compute the height of buildings using interferometric methods, and to compare the results with the classic layover method. Second, we will study the coherence and the entropy of polarimetric images and classify lands according to their nature : vegetation, ocean, city. We will finally try to retrieve the central frequency of acquired images in both band X and L given the values of pixel resolution.

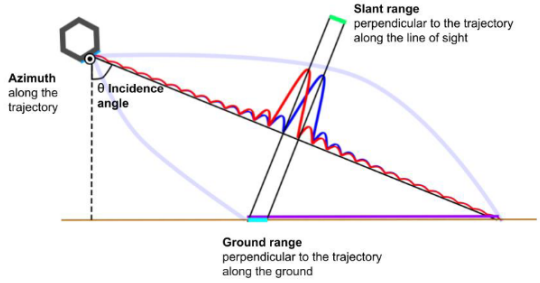

Fig. 1: Geometry of SAR imaging

The file `Ville1.npz` contains:

1. A matrix (`parametre_image`) of size $N_r \times N_c \times 4$, which represents a temporally aligned stack of 4 images acquired by the TerraSAR-X satellite (X-band, wavelength of 3.1 cm, parameter `l_onde`).
2. The acquisition dates, provided as a character string in the format `YYYYMMDD` (parameter `vec_date`).
3. The baselines between the 2nd, 3rd, and 4th acquisitions relative to the first, which is considered the reference (parameter `vec_baseline`).
4. The satellite's flight altitude, which is 514 km (parameter `H`).
5. The incidence angle in degrees (parameter `theta`).
6. The pixel size in metesrs:
    - In slant range (parameter `taille_pixel_slantrange`), corresponding to the image columns.
    - In azimuth (parameter `taille_pixel_azimut`), corresponding to the image rows.

2. Building height : interferometry or layover ?

The modulus of the interferometric image shows values ranging from 0 to 1. It is computed using the provided function `interfero` which computes the modulus and the phase of the interferometric image. Because this function uses tthe convolution of the element-wize product of the pixels of a first image with the complex conjugate of the pixels of the second one, it computes the correlation of the two pictures : 0 values are then pixels that are not correlated, and 1 values are pixels that are perfectly correlated.

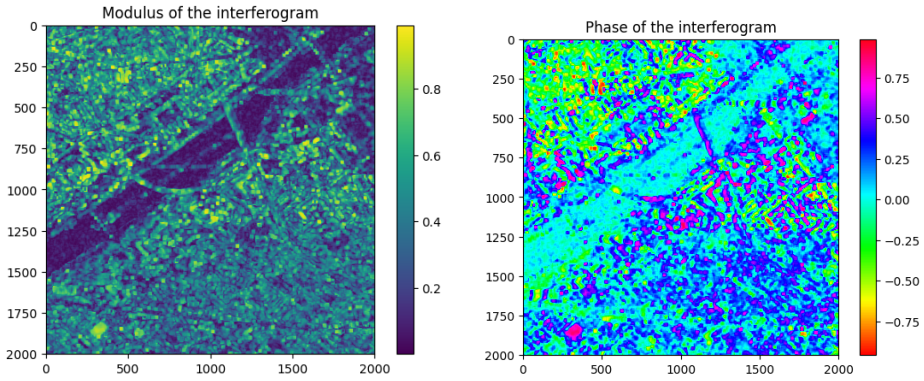

(a) Modulus (b) Phase

Fig. 2: Modulus and Phase of interferometric image

Because we need to take a local average of the pixels, the image is blurry and it is hard to distinguish changes from fake alarms.

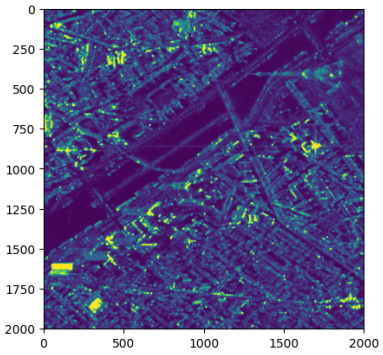

Fig. 3: Ratio of images' modulus

The map computed from the ratio of the modulus of the two images is less blurry and therefore more relevant for change search. We did not find a suitable threshold to apply to the interferogram, even 0.95 was not relevant, with multiple brights spots remaining and that could not be related to those obtained with the ratio of the modulus.

Layover

From [1] we can retrieve the formula giving the height of a building from the layover method. The height h of a building is given by :

$$h = dn \times pix_{slant} \tag{1}$$

This leads to a height of 244,17 m for the Eiffel tower, which is 324 m tall, and 48,65 m for the Mirabeau tower, which is 70 m tall. The difference of 25-30% can be linked with the difficulty to find the exact pixel where the top of the building is located, and potential innacurracy within the pixel slant size.

Interferometry

in this method, the heights of the buiilding can be related to the phase of the interferogram through the formula :

$$h = \frac{\Delta\Phi}{kz}, \qquad kz = 4\pi \times baseline/\lambda/H/tan(\theta) \tag{2}$$

The interferometric fringes appears because of the baseline Geometry: the spatial separation (baseline) between the radar sensors affects the phase difference due to slightly different viewing angles. Here we actualy sees alternating bright and dark fringes onto the Eiffel tower, and the Mirabeau tower (but less clearly visible), which are the result of constructive and destructive interference between the two images.

The numpy wrap function offers to ccompute the modulo of a serie of value in order for them to never exceed a given value called the period, and compute the correct value so that the difference between two adjacent values never exceed another value called the discont value. Here, we did not succeed in using this function so we ploted the phase (multiplied by a factor 10) and manually counted the elapsed phase.

We then can compute the height of the buildings : given the baseline between the four images : `[ 0. 120.22 -13.385 -104.426]`, the periods of the phases : 3π for Mirabeau and $1\pi 1$ for the Eiffel tower, we get 252,28 m for the Eiffel tower and 68,8 m for the Mirabeau tower,

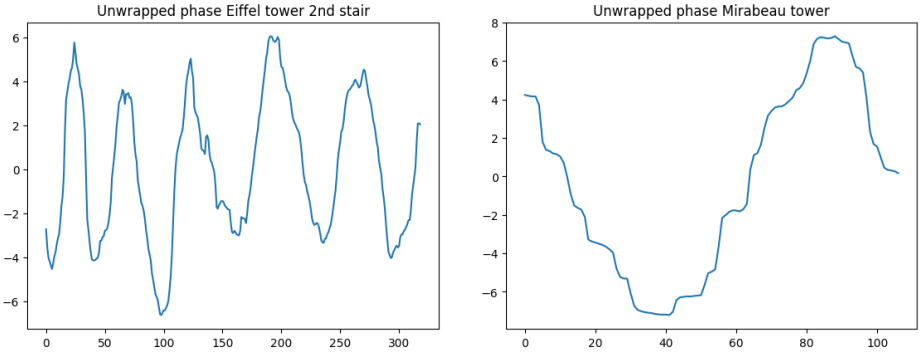

(a) Eiffel tower 2nd stair (b) Mirabeau tower

Fig. 4: Wrapped phase of interferometric image

which are clearly closer to the real values. the resulting difference can be partly explained by the deformation of the buildings, given by the formula:

$$dr = dphi - kz * h/4/\pi/\lambda \tag{3}$$

We get a deformation of 34 m for the Eiffel tower and 9 m for the Mirabeau tower.

3. Multi-temporal pile : polarimetric classification

The file `Ville2.mat` contains the 3 polarimetric channels (HH, HV, and VV) of an image acquired with the Radarsat-2 satellite (C-band, wavelength 5cm). Polarimetry allows obtaining information on backscattering mechanisms and better discriminating the elements present in the scene. Below are shown the Lexico and the Pauli RGB representation of the concatenated polarized channels.

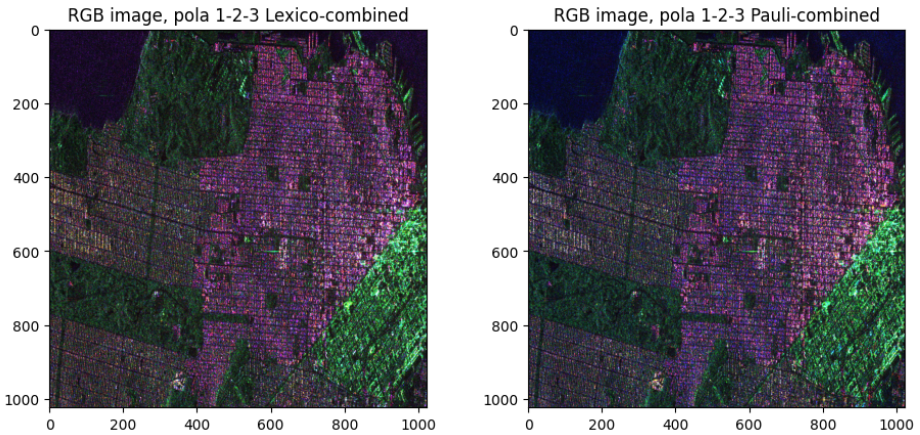

(a) Lexico representation (b) Pauli representation

Fig. 5: Representation of a polarimetric image

The biggest difference between the two images is visible on the vegetation and the sea, where the details are more accurately represented and the rresolution is bettern with less noise on the Pauli representation. Indeed, in the code, the Lexico function just create a 3 channel RGB image base on the threshSAR computed arrays from the image, when in the Pauli function, the output is generated from the difference and the sum of the channel 1 and 3, with channel 1 counting twice. This allows to better discriminate the different elements of the image.

By looking at the RGB Pauli representation, we would suggest to classify the lands among three parts : the sea (blue), the vegetation (dark green), and the city (red and bright green).

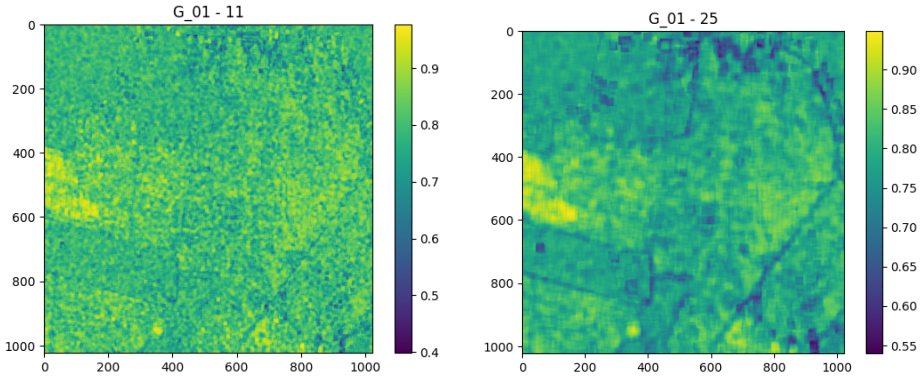

(a) WindowShape = 11 (b) WindowShape = 25

Fig. 6: Coherence between channels 1 and 2 for different window shapes

We can then compute an equivalent of the usual covariance matrix. In fact, each pixel of the image is a 3 dimensional vector, so the function computes the covariance matrix for that vector and for each pixel of the image. In the `boxcarFilterMultichannel`, the value of the `windowShape` parameter takes the same role as the dimension of the convolution kernel acting as the low pass filter, which were averaging the neighboured pixels, in the `fonctionfiltreMoyen` function. Diminishing this value leads to smaller diagonal values in the covariance matrices within the computed matrix. It also leads to a better discrimination of the different contours of the different zones that we observed earlier, in tyhe coherence map computed according to the formula :

$$\gamma_{1,2} = \frac{C(1,2)}{\sqrt{C(1,1)C(2,2)}} \tag{4}$$

Here, windowshape = 25 seems a good value in this purpose.

Thanks to the `CloudePottierDecompositionImage` function, we can compute the entropy and the alpha value of the image. From the code, we deducted the formula giving the entropy :

$$S = \frac{xlog(x) + ylog(y) + zlog(z)}{log(n)} \tag{5}$$

with $x = \lambda_1/S$ and $S = \lambda_1 + \lambda_2 + \lambda_3$ the eigenvalues of the singuar decomposition of the covariance matrix of each pixel, and n their dimension (3 here).

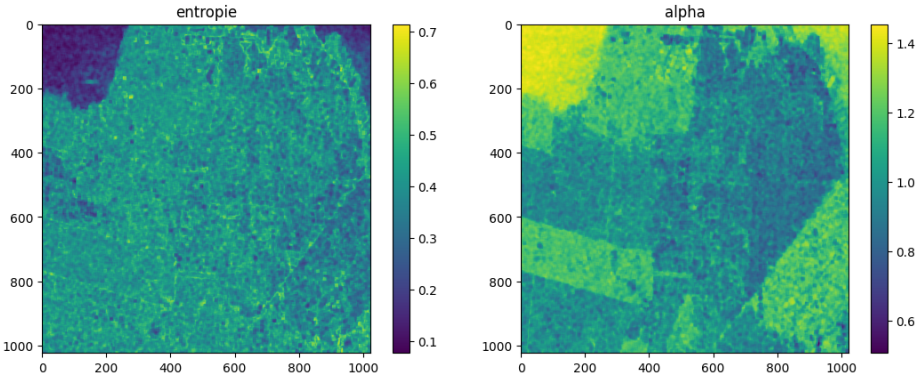

(a) entropy (b) alpha

Fig. 7: Computed entropy and alpha maps for classification

The calculation of entropy only allows for the segregation of sea from land, with a threshold close to 0.3. However, the calculation of the alpha value allows for the segmentation of sea and vegetation with a threshold set close to 1.3, and also segregates buildings with a threshold set at 1.1.

These measurements are difficult to relate to the threshold values proposed by Cloude and Pottier since their alpha scale ranges from 0 to 90, whereas our scale ranges from 0.7 to 1.4. Nevertheless, we can attribute the sea to zone Z9 and the land to zone Z6:

Zone 9: Low Entropy Surface Scatter
Zone 8: Low Entropy Dipole Scattering
Zone 7: Low Entropy Multiple Scattering Events
Zone 6: Medium Entropy Surface Scatter
Zone 5: Medium Entropy Vegetation Scattering
Zone 4: Medium Entropy Multiple Scattering
Zone 3: High Entropy Surface Scatter
Zone 2: High Entropy Vegetation Scattering
Zone 1: High Entropy Multiple Scattering

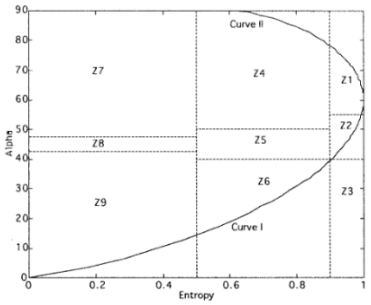

Fig. 4. Feasible region in α-H plane for random media scattering problems.

Fig. 8: Cloude and Pottier classification

4. Central frequency of the acquired images

Here we simpoly plot the two polarimetric images using Pauli's representation but we will not be able to compute the central frequency of the images.

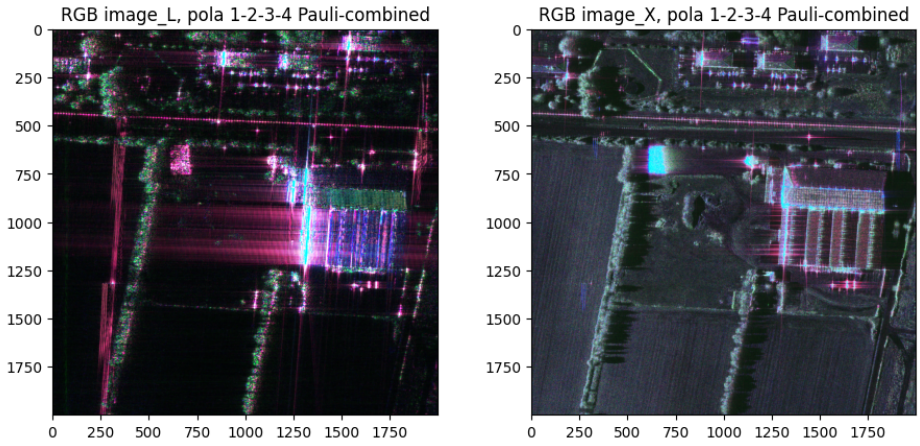

(a) Bandwidth L (b) Bandwidth X

Fig. 9: Bandwidth X and L of a polarimetric image

Below we plot the differences between the polarimetric channels of the two bandwidths. In orange are the pixels that are present in the first image, of bandwidth L, and in blue, those which are resent in the X bandwidth image. the image of bandwidth X is of so much better resolution.

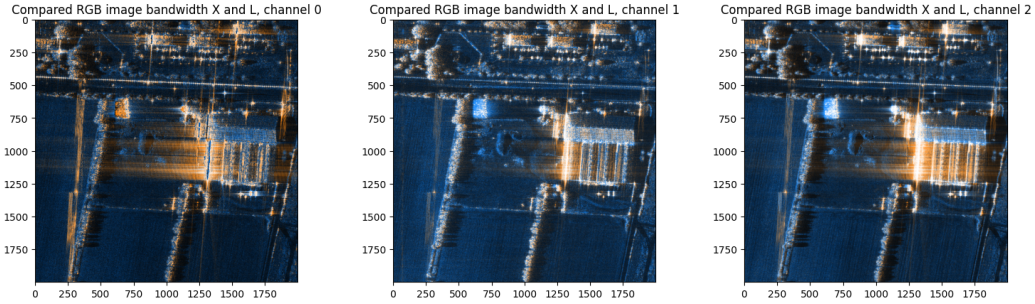

(a) Channel 0 (b) Channel 1 (c) Channel 2

Fig. 10: Difference between the polarization channel of the two bandwidth

5. Conclusion

In conclusion, this study demonstrated the use of Synthetic Aperture Radar (SAR) imaging for building height estimation, polarimetric classification, and central frequency analysis (work in progress). By employing interferometric methods and layover techniques, we were able to estimate building heights with reasonable accuracy, and able to highlight the accuracy of the interferometric method. The use of polarimetric data allowed for effective land classification, distinguishing between sea, vegetation, and urban areas, thanks to the computation of polarimetric coherence, of entropy and related alpha. Although we faced challenges in computing the central frequency, the analysis provided valuable insights into the differences between L and X bandwidth images. Overall, SAR imaging proves to be a powerful tool for environmental monitoring and urban planning, offering detailed and reliable information over time.

List of Figures